

# Evidence for $\pi^+\pi^-$ scattering in $p + p$ collisions at $\sqrt{s_{NN}} = 200$ GeV

**P. Fachini, R. S. Longacre, Z. Xu and H. Zhang**

Brookhaven National Laboratory, Upton, NY, 11973, USA

E-mail: pfachini@bnl.gov

**Abstract.**  $\rho(770)^0$  mass shift of about  $-40$  MeV/ $c^2$  was measured in  $p + p$  collisions at  $\sqrt{s_{NN}} = 200$  GeV at RHIC. Previous mass shifts have been observed at CERN and LEP. We will show that phase space does not account for the  $\rho(770)^0$  mass shift measured at RHIC, CERN and LEP and conclude that there are significant scattering interactions in  $p + p$  collisions.

## 1. Introduction

In-medium modification of the  $\rho$  meson due to the effects of increasing temperature and density has been proposed as a possible signal of a phase transition of nuclear matter to a deconfined plasma of quarks and gluons, which is expected to be accompanied by the restoration of chiral symmetry [1].

The  $\rho^0$  meson measured in the dilepton channel probes all stages of the system formed in relativistic heavy-ion collisions because the dileptons have negligible final state interactions with the hadronic environment. Heavy-ion experiments at CERN show an enhanced dilepton production cross section in the invariant mass range of 200-600 MeV/ $c^2$  [2]. The hadronic decay measurement at RHIC [3],  $\rho(770)^0 \rightarrow \pi^+\pi^-$ , was the first of its kind in heavy-ion collisions. Since the  $\rho^0$  lifetime of  $c\tau = 1.3$  fm is small with respect to the lifetime of the system formed in Au+Au collisions, the  $\rho^0$  meson is expected to decay, regenerate, and rescatter all the way through kinetic freeze-out. Therefore, the measured  $\rho^0$  mass at RHIC should reflect conditions at the late stages of the collisions [4, 5]. However, it has been shown that the  $\rho^0$  width goes to zero with the  $\rho^0$  mass dropping near the chiral phase transition, which is called the vector manifestation and it can occur near  $T_c$  in the hot and dense matter [6]. In this scenario, the  $\rho^0$  lifetime becomes very large and the  $\rho^0$  produced at the early stages can also be measured in the hadronic channel.

At RHIC, the  $\rho^0$  was measured in peripheral Au+Au and minimum bias  $p + p$  collisions, where a mass shift of -70 and -40 MeV/ $c^2$  of the position of the  $\rho^0$  was observed [3]. The possible explanations for the apparent modification of the  $\rho^0$  meson properties were attributed to dynamical interactions with the surrounding matter, interference between various  $\pi^+\pi^-$  scattering channels, phase space distortions due to the rescattering of pions forming  $\rho^0$  and Bose-Einstein correlations between  $\rho^0$  decay daughters and pions in the surrounding matter.

The modification of the  $\rho^0$  properties in heavy-ion collisions has been expected [1]. The modification observed in  $p + p$  collisions at RHIC has been measured before at CERN and LEP. Until now, the mass shift measured in  $p + p$  has been attributed to phase space. In this paper, we will show that phase space does not account for the  $\rho(770)^0$  mass shift measured at RHIC [3], CERN [7] and LEP [8, 9, 10, 11] and conclude that there are significant scattering interactions in  $p + p$  collisions.

## 2. Discussion $\rho$ mass average from the Particle Data Group (PDG)

We will first discuss the  $\rho$  mass average from the PDG [12]. The  $\rho^0$  mass average  $775.8 \pm 0.5$  MeV/ $c^2$  from  $e^+e^-$  was obtained from either  $e^+e^- \rightarrow \pi^+\pi^-$  or  $e^+e^- \rightarrow \pi^+\pi^-\pi^0$ . This means that the  $\rho^0$  mass average was obtained from *exclusive leptonic reactions*. Similarly, the  $\rho^\pm$  mass average  $775.5 \pm 0.5$  MeV/ $c^2$  was also obtained from *exclusive leptonic reactions*.

The  $\rho$  averages reported by the PDG from reactions other than leptonic interactions

are systematic lower than the value obtained from *leptonic exclusive interactions* by  $\sim 10$  MeV/ $c^2$  [12]. The  $\rho$  production in these hadronic reactions are inclusive and exclusive. In the case of inclusive productions, the phase space was taken into account when the  $\rho$  mass was measured (e.g. [7]).

These observations lead us to conclude that the  $\rho$  mass depends on specific interactions, e.g. whether the  $\rho$  is produced in inclusive or exclusive reactions. Since a leptonic reaction and exclusive measurement of the  $\rho^0$  lead to a negligible modification of any kind of the  $\rho^0$  mass, the average  $775.8 \pm 0.5$  MeV/ $c^2$  [12] from  $e^+e^-$  should correspond to the  $\rho^0$  mass in the vacuum.

### 3. $\rho^0$ mass shifts at RHIC, CERN, and LEP

The  $\rho^0$  was measured in the hadronic decay channel  $\rho^0 \rightarrow \pi^+\pi^-$  at RHIC, CERN, and LEP in inclusive production. At RHIC, the STAR collaboration measured the  $\rho^0$  at  $\sqrt{s_{NN}} = 200$  GeV and observed mass shifts of the position of the  $\rho^0$  peak of about -40 MeV/ $c^2$  and -70 MeV/ $c^2$  in minimum bias  $p + p$  and peripheral Au+Au collisions, respectively [3]. The invariant mass distributions from [3] is shown in Fig. 1. The STAR collaboration took into account the phase space (PS) [4, 13, 14, 15, 16, 17, 18, 19, 20] and the  $\rho^0$  distribution was fit to the BW $\times$ PS function [3], where BW is the relativistic Breit-Wigner function [3]. The  $\rho^0$  mass obtained from the BW $\times$ PS fit is depicted in Fig. 2, where it is clear that the phase space did not account for the measured mass shifts of the position of the  $\rho^0$  peak.

The  $K^*(892)$  was also measured at RHIC by the STAR collaboration and a mass shift of  $\sim 10$  MeV/ $c^2$  was observed for  $p_T < 1$  GeV/ $c^2$  [21]. Previous experiments have not observed a mass shift for the  $K^*(892)$ , for a review see [12]. However, these experiments have not performed the detailed study of the  $K^*$  mass that the STAR collaboration achieved [21]. Actually, these previous experiments reported the  $K^*$  mass *integrated* in  $p_T$ ,  $x_F$ , or  $x_p$  [12].

At CERN, NA27 measured the  $\rho^0$  in minimum bias  $p + p$  at  $\sqrt{s} = 27.5$  GeV and reported a mass of  $762.6 \pm 2.6$  MeV/ $c^2$  [7]. The invariant  $\pi^+\pi^-$  mass distribution after subtraction of the mixed-event reference distribution that was fit to the BW $\times$ PS function in [7] is shown in Fig. 3. The vertical dashed line represent the average of the  $\rho^0$  mass  $775.8 \pm 0.5$  MeV/ $c^2$  measured in  $e^+e^-$  [12]. The vertical solid line is the  $\rho^0$  mass  $762.6 \pm 2.6$  MeV/ $c^2$  reported by NA27 [7]. As shown in Fig. 3, the position of the  $\rho^0$  peak is shifted by  $\sim 30$  MeV/ $c^2$  compared to the  $\rho^0$  mass in the vacuum  $775.8 \pm 0.5$  MeV/ $c^2$  [12]. The shift of the  $\rho^0$  peak can be quantified by fitting the NA27  $\pi^+\pi^-$  mass distribution after subtraction of the mixed-event reference distribution to the BW function in [3]. The fit is depicted in Fig. 4 and the value of the maximum of the distribution obtained from the fit is  $747.6 \pm 2.0$  MeV/ $c^2$  with  $\chi^2/ndf = 1.9$ .

As mentioned, NA27 obtained the  $\rho^0$  mass by fitting the invariant  $\pi^+\pi^-$  mass distribution to the BW $\times$ PS function, and they reported a mass of  $762.6 \pm 2.6$  MeV/ $c^2$ , which is  $\sim 10$  MeV/ $c^2$  lower than the  $\rho^0$  mass in the vacuum. Ideally, the PS factor

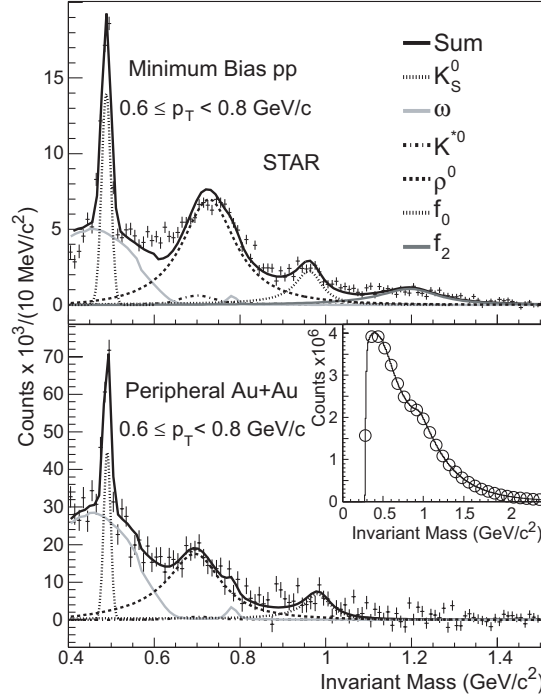


**Figure 1.** The raw  $\pi^+\pi^-$  invariant mass distributions after subtraction of the like-sign reference distribution for minimum bias  $p + p$  (top) and peripheral Au+Au (bottom) interactions measured by STAR. For details see [3]

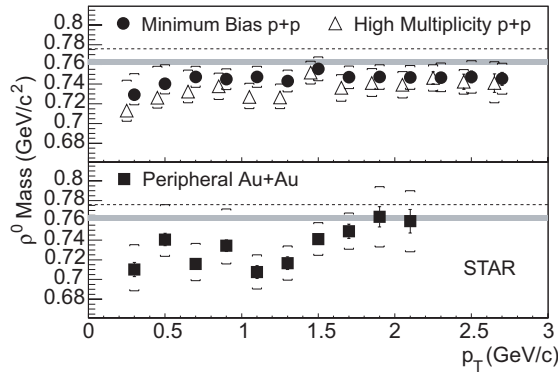


**Figure 2.** The  $\rho^0$  mass as a function of  $p_T$  for minimum bias  $p + p$  (filled circles), high multiplicity  $p + p$  (open triangles), and peripheral Au+Au (filled squares) collisions measured by STAR. The error bars indicate the systematic uncertainty. Statistical errors are negligible. The  $\rho^0$  mass was obtained by fitting the data to the BW $\times$ PS functional form described in [3]. The dashed lines represent the average of the  $\rho^0$  mass measured in  $e^+e^-$  [12]. The shaded areas indicate the  $\rho^0$  mass measured in  $p + p$  collisions [7]. The open triangles have been shifted downward on the abscissa by 50 MeV/c for clarity.

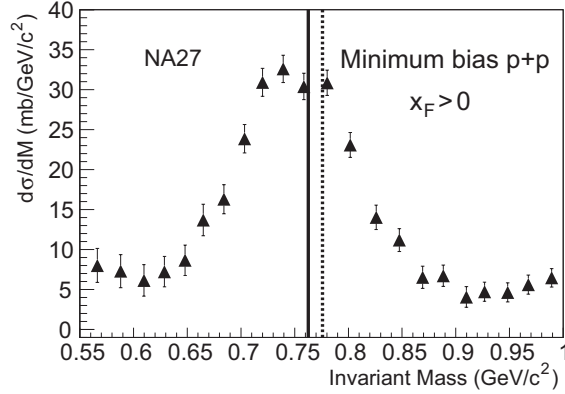


**Figure 3.** The invariant  $\pi^+\pi^-$  mass distribution after subtraction of the mixed-event reference distribution for minimum bias  $p + p$  collisions measured by NA27. For details see [7]. The vertical dashed line represent the average of the  $\rho^0$  mass  $775.8 \pm 0.5$  MeV/ $c^2$  measured in  $e^+e^-$  [12]. The vertical solid line is the  $\rho^0$  mass  $762.6 \pm 2.6$  MeV/ $c^2$  reported by NA27 [7].

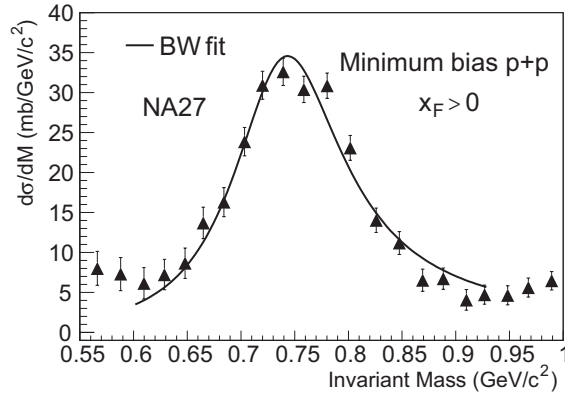


**Figure 4.** The invariant  $\pi^+\pi^-$  mass distribution after subtraction of the mixed-event reference distribution for minimum bias  $p + p$  collisions measured by NA27 [7] fit to the BW function in [3]. For details see [7].

should have accounted for the shift on the  $\rho^0$  peak, and the mass obtained from the fit should have agreed with the  $\rho^0$  mass in the vacuum. However, this was not the case, since the phase space did not account for the mass shift on the position of the  $\rho^0$  peak.

At LEP, OPAL, ALEPH, and DELPHI measured the  $\rho^0$  in inclusive  $e^+e^-$  reactions at  $\sqrt{s} = 90$  GeV [8, 9, 10, 11]. Even though OPAL never reported the value of the  $\rho^0$  mass, OPAL reported a shift on the position of  $\rho^0$  peak by  $\sim 70$  MeV/ $c^2$  at low  $x_p$  and no shift at high  $x_p$  ( $x_p \sim 1$ ) [8, 9]. OPAL also reported a shift in the position of the  $\rho^\pm$  peak from -10 to -30 MeV/ $c^2$ , which was consistent with the  $\rho^0$  measurement [8, 9]. ALEPH reported the same shift on the position of  $\rho^0$  peak observed by OPAL [10]. DELPHI fit the invariant  $\pi^+\pi^-$  mass distribution after background subtraction to the BW $\times$ PS function in a particular  $x_p$  region ( $0.1 < x_p < 0.4$ ) and reported a  $\rho^0$  mass of  $757 \pm 2$  MeV/ $c^2$  [11], which is five standard deviations below than the  $\rho^0$  mass in

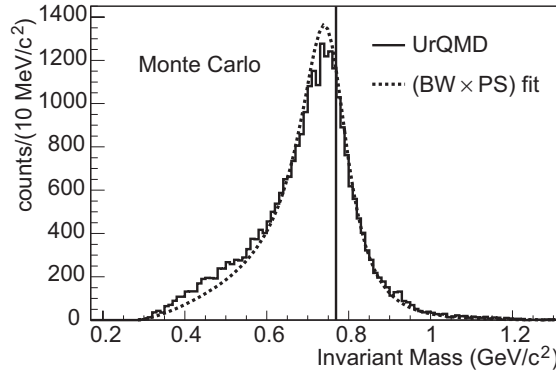


**Figure 5.**  $\rho^0$  distribution (solid line) from  $10^5$  central ( $b < 3fm$ ) Au+Au UrQMD events at  $\sqrt{s_{NN}} = 200$  GeV for  $0.2 \leq p_T < 0.4$  at  $|y| \leq 0.5$ . The vertical solid line is the input value of  $769 \text{ MeV}/c^2$  for the  $\rho^0$  mass in UrQMD. The dashed line is the fit to the BW $\times$ PS function [3].

the vacuum ( $775.8 \pm 0.5 \text{ MeV}/c^2$ ). Bose-Einstein correlations were used to describe the shift on the position of  $\rho^0$  peak. However; high (even unphysical) chaoticity parameters ( $\lambda \sim 2.5$ ) were needed [8, 9, 10].

#### 4. Phase space in Au+Au collisions

In Au+Au collisions, the phase space accounts for hadrons scattering and resonance regeneration. Since the pions have a momentum distribution, this will cause a distortion in the  $\rho^0$  spectral shape due to phase space. In the case of the  $\rho^0$ ,  $\pi^+\pi^- \rightarrow \rho^0 \rightarrow \pi^+\pi^-$ . The effect of the phase space on the  $\rho^0$  mass distribution can be studied using transport model calculations, such as UrQMD [18]. UrQMD only has the imaginary part of the scattering cross section, which means that there is no medium modification in the calculation. The evolution of the hadron in UrQMD depends solely on scattering cross-sections. Figure 5 depicts the  $\rho^0$  distribution (solid line) from  $10^5$  central ( $b < 3fm$ ) Au+Au UrQMD events at  $\sqrt{s_{NN}} = 200$  GeV for  $0.2 \leq p_T < 0.4$  at midrapidity ( $|y| \leq 0.5$ ). The vertical solid line is the input value of  $769 \text{ MeV}/c^2$  for the  $\rho^0$  mass in UrQMD. A shift of  $\sim 30 \text{ MeV}$  on the position of the  $\rho^0$  peak is observed. The dashed line in Fig. 5 is the fit to the BW $\times$ PS function [3] and the mass of  $765 \text{ MeV}/c^2$  obtained from the fit is equivalent to the input value of  $769 \text{ MeV}/c^2$ .

#### 5. Phase space in $p + p$ collisions

In  $p+p$  collisions, most models assume that particles are born at hadronization according to phase space without any final state interaction. In multiparticle production processes, single-inclusive (e.g.  $p + p$ ), invariant particle spectra are typically exponential in  $p_T$  [22]. The exponential behavior does not require final state interactions and it can be due to phase space population at hadronization. The slope parameter in  $p + p$  collisions

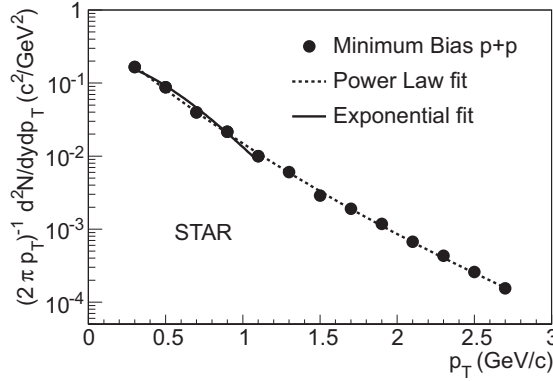


**Figure 6.** The  $p_T$  distribution at  $|y| < 0.5$  for minimum bias  $p + p$  collisions [3]. The black circles are the data, the dashed line is the power-law fit and the solid line is the exponential fit. See [3] for the fit functions. The errors shown are statistical only and smaller than the symbols.

are independent of the particle species [23]. At RHIC, the  $\rho^0$  spectra in minimum bias and high multiplicity  $p + p$  are exponential in  $p_T$  up to  $1.1 \text{ GeV}/c^2$  with slope parameters of  $\sim 180 \text{ MeV}$ . The  $\rho^0$  spectrum in minimum bias  $p + p$  [3] is depicted in Fig. 6. For reference, the slope parameter of  $\pi^-$  is  $\sim 160 \text{ MeV}$  [24]. Note that the slope parameter in  $p + p$  is independent of the particle rest mass and shows  $m_T$  scaling. These results also are independent of the multiplicity.

However, the  $\rho^0$  mass measured in  $p + p$  at RHIC is multiplicity dependent (the mass shift in high multiplicity is higher than in minimum bias  $p + p$  collisions) [3], which is opposite to the slope parameter that is multiplicity independent. We will demonstrate that the mass should be independent of  $p_T$  as well as multiplicity at hadronization without final state interactions. According to quantum mechanics, a resonance at rest is described by the wave function,

$$\Psi(x, t) \propto \exp\left(\frac{-iE_0 t}{\hbar}\right) \exp\left(\frac{-t}{2\tau}\right) \quad (1)$$

where  $\tau$  is the lifetime and  $E_0$  is the energy at rest. The probability amplitude of the resonance decay can be written as

$$\tilde{\Psi}(E, x) \propto \int_0^\infty \left(\exp\left(\frac{-iEt}{\hbar}\right)\right)^* \Psi(x, t) dt \quad (2)$$

$$\tilde{\Psi}(E, x) \propto \frac{1}{i\frac{E-E_0}{\hbar} - \frac{1}{2\tau}} \Psi(x) \quad (3)$$

$$P(E) \propto \left|\frac{1}{i\frac{E-E_0}{\hbar} - \frac{1}{2\tau}}\right|^2 \int |\Psi(x)|^2 dx \quad (4)$$

$$P(E) \propto \frac{\Gamma/2}{(E - E_0)^2 + \frac{\Gamma^2}{4}} \quad (5)$$

where  $\Gamma = \hbar/\tau$ , and the probability amplitude is a non-relativistic Breit-Wigner distribution. Besides the Breit-Wigner distribution there should be the phase space

due string fragmentation that is also independent of  $p_T$  and multiplicity. Equation 5 above should have a phase space of  $\exp(\frac{-m_T}{T})$ , where  $m_T$  equals  $\sqrt{E^2 + p_T^2}$  and  $T$  equals 160 MeV. Equation 5 is then rewritten as

$$P(E, p_T) \propto \frac{\Gamma/2}{(E - E_0)^2 + \frac{\Gamma^2}{4}} \exp(\frac{-m_T}{T}) \quad (6)$$

Fig. 5 is a very good example of this phase space distortion. However; as discussed previously, the phase space does not describe the mass shift of the  $\rho$  meson measured at RHIC, CERN, and LEP.

Most event generators (e.g. PYTHIA [25] and HIJING [26]) create resonances according to a non-relativistic Breit-Wigner function at a given  $p_T$ . However, we showed that this is not consistent with quantum mechanics, and a more reasonable way to produce resonances is to use equation 6 instead of a non-relativistic Breit-Wigner function at a fixed  $p_T$ .

Since the phase space of the final multiparticle state *cannot* explain the distortion of the  $\rho^0$  line shape, we can conclude that the phase space in  $p+p$  collisions also accounts for hadrons scattering and forming resonances. In the case of the  $\rho^0$ ,  $\pi^+\pi^- \rightarrow \rho^0 \rightarrow \pi^+\pi^-$ . This can be pictured in the string fragmentation particle production scenario, where the string breaks several times, two pions are formed, they scatter, and form a  $\rho^0$ . Such interactions are significant and modify the  $\rho^0$  spectral shape in  $e^+e^-$  and  $p + p$  from a relativistic  $p$ -wave Breit-Wigner function.

Using the  $p + p$  data from the top plot of Fig. 1 and the rescattering formalism of [27], we can test the ideas of a mass shift having a  $\pi^+\pi^-$  scattering componet. The di-pion production is given by equation 21 of [27]. For the  $\rho^0$  which is  $p$ -wave  $\ell = 1$  equation 21 becomes

$$|T|^2 = |D|^2 \frac{\sin^2(\delta_1)}{q^3} + \frac{|A|^2}{q^3} |\alpha \sin(\delta_1) + q^3 \cos(\delta_1)|^2 \quad (7)$$

The  $\delta_1$  is the  $p$ -wave phase shift ( $\rho^0$ ) and  $\frac{\sin^2(\delta_1)}{q^3}$  in our case becomes the Breit-Wigner times phase space equation 6.  $|D|^2$  becomes the direct production of  $\rho^0$  for the  $p_t$  range 600 to 800 MeV/c.  $|A|^2$  is the phase space overlap of di-pions in the  $\ell = 1$  partial waves. The pions emerge from a close encounter in a defined quantum state with a random phase. The emerging pions can re-interact or re-scatter through the  $p$ -wave quantum state or a phase shift. The phase space overlap comes from sampling the  $\pi$  spectrum from  $p + p$  collisions, where the sum of the  $\pi^+\pi^-$  has the correct  $p_t$  range. The di-pion mass spectrum for this  $p_t$  range falls with increasing di-pion invariant mass( $E$ ). The variable  $\alpha$  is related to the real part of the di-pion rescattering diagram and measures the range of interaction [27]. There is a problem with equation(8), in which the  $p$ -wave phase space  $q^3$  should be modified so it goes to 1 as  $E \rightarrow \infty$ . Equation 7 becomes

$$|T|^2 = |D|^2 \frac{\sin^2(\delta_1)}{PS'} + \frac{|A|^2}{PS'} |\alpha \sin(\delta_1) + PS' \cos(\delta_1)|^2 \quad (8)$$

where

$$PS' = \frac{2q(q/q_0)^2}{\frac{E(q/q_0)^2}{(1+(q/q_0)^2)}} \quad (9)$$



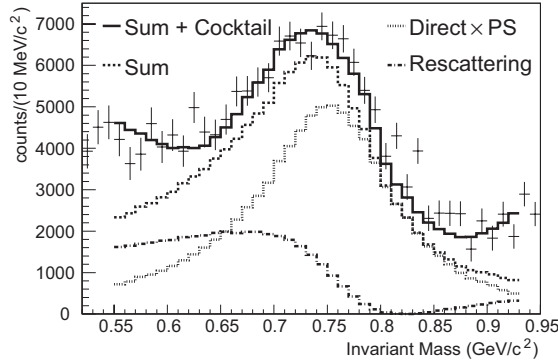


**Figure 7.** Fit to the data using equation 8 (solid line), the direct  $\rho^0$  contribution term times the phase space (dashed line), the rescattering term (dash-dotted line) and the sum of the both (dashed line).

is a better  $PS'$  factor  $\alpha$  and can be related to the range of scattering.

$$\alpha = \left(1.0 - \frac{r^2}{r_0^2}\right) \quad (10)$$

The  $r$  is the radius of rescattering in fermis and  $r_0$  is 1.0 fermi or the limiting range of the strong interaction. We also use the 1.0 fermi distance to set  $q_0$  at 200 MeV/ $c$ .

In order to fit the  $p + p$  data we need to add the rest of the cocktail of resonances used by STAR [3]. Such a fit is shown in Fig. 7 (solid line), where the direct  $\rho^0$  term times the phase space (dotted line) and the rescattered term (dash-dotted line) plus the sum (dashed line) are also depicted. The value for  $\alpha$  from the fit is 0.47, which implies  $r = 0.73$  fermi.

We see that the mass shift is a unitary effect modifying a  $\pi\pi$  source which is not the  $\rho$ . This  $\pi\pi$  source becomes a  $\rho$  through reinteraction. The mass shift of the  $\rho$  seen in [28] is due to the same unitary effect, except that the direct production of the  $\rho$  in this case is coherent with the  $\pi\pi$  source.

## 6. Conclusions

We discussed that the natural mass of the  $\rho$  meson should be measured in *exclusive* reactions only. We showed that a shift on the position of the  $\rho^0$  peak has been measured before and that the phase space does not account for the  $\rho(770)^0$  mass shift measured at RHIC, CERN, and LEP. In addition, we discussed the phase space in  $p + p$  collisions and concluded that there are significant scattering interactions in  $p + p$  reactions. These interactions modify the  $\rho^0$  line shape in  $p + p$  and  $e^+e^-$  interactions from a Breit-Wigner function. Using the rescattering formalism of [27], we can reproduce the  $\rho^0$  mass shift measured by the STAR collaboration in minimum bias  $p + p$  collisions.

## 7. Acknowledgement

This work was supported in part by the HENP Divisions of the Office of Science of the U.S. DOE.

- [1] R. Rapp and J. Wambach, Adv. Nucl. Phys. **25**, 1 (2000).
- [2] G. Agakishiev *et al.*, Phys. Rev. Lett. **75**, 1272 (1995); B. Lenkeit *et al.*, Nucl. Phys. A **661**, 23 (1999).
- [3] J. Adams *et al.*, Phys. Rev. Lett. **92** 092301 (2004).
- [4] E.V. Shuryak and G.E. Brown, Nucl. Phys. A **717**, 322 (2003).
- [5] R. Rapp, Nucl. Phys. A **725**, 254 (2003).
- [6] M. Harada and K. Yamawaki, Phys. Rept. **381**, 1 (2003).
- [7] M. Aguilar-Benitez *et al.*, Z. Phys. C **50**, 405 (1991).
- [8] P.D. Acton *et al.*, Z. Phys. C **56**, 521 (1992).
- [9] G.D. Lafferty, Z. Phys. C **60**, 659 (1993); (private communication).
- [10] D. Buskulic *et al.*, Z. Phys. C **69**, 379 (1996).
- [11] K. Ackerstaff *et al.*, Eur. Phys. J. C **5**, 411 (1998).
- [12] S. Eidelman *et al.*, Phys. Lett. B **592**, 1 (2004).
- [13] H.W. Barz *et al.*, Phys. Lett. B **265**, 219 (1991).
- [14] P. Braun-Munzinger (private communication).
- [15] P.F. Kolb and M. Prakash, nucl-th/0301007.
- [16] R. Rapp, Nucl. Phys. A **725**, 254 (2003).
- [17] W. Broniowski *et al.*, Phys. Rev. C **68**, 034911 (2003).
- [18] M. Bleicher and H. Stöcker, J. Phys. G **30**, S111 (2004).
- [19] S. Pratt and W. Bauer, Phys. Rev. C **68**, 064905 (2003).
- [20] P. Granet *et al.*, Nucl. Phys. B **140**, 389 (1978).
- [21] J. Adams *et al.*, Phys. Rev. C **71** 064902 (2005).
- [22] R. Hagedorn, Relativistic Kinematics, W.A. Benjamin, 1963; E. Byckling and K. Kajantie, Particle Kinematics, Wiley, 1973.
- [23] I.G. Bearden *et al.*, Phys. Rev. Lett. **78** 2080 (1997).
- [24] J. Adams *et al.*, Phys. Rev. Lett. **92** 112301 (2004). Wesley, 1985.
- [25] T. Sjöstrand *et al.*, hep/0308153 (2003).
- [26] X.N. Wang and M. Gyulassy, Phys. Rev. D **44**, 3501 (1991); Compt. Phys. Commun. **83**, 307 (1994).
- [27] Ron S. Longacre, nucl-th/0303068 (2003).
- [28] J. Adams *et al.*, Phys. Rev. Lett. **89** 272302 (2002).